

Isospin mixing of the isobaric analog state studied in a high-resolution $^{56}\text{Fe}(^3\text{He}, t)^{56}\text{Co}$ reaction

H. Fujita,^{1,2,*} Y. Fujita,^{3,4} T. Adachi,⁴ H. Akimune,⁵ N. T. Botha,⁶ K. Hatanaka,⁴ H. Matsubara,^{4,†} K. Nakanishi,⁴ R. Neveling,⁷ A. Okamoto,⁵ Y. Sakemi,^{4,‡} T. Shima,⁴ Y. Shimizu,^{4,§} F. D. Smit,⁷ T. Suzuki,⁴ A. Tamii,⁴ and M. Yosoi⁴

¹*School of Physics, University of the Witwatersrand, Johannesburg 2050, South Africa*

²*iThemba LABS, National Research Foundation, Somerset West 7129, South Africa*

³*Department of Physics, Osaka University, Toyonaka, Osaka 560-0043, Japan*

⁴*Research Center for Nuclear Physics (RCNP), Ibaraki, Osaka 567-0047, Japan*

⁵*Department of Physics, Konan University, Kobe, Hyogo 658-8501, Japan*

⁶*Department of Physics, University of Cape Town, Rondebosch 7701, South Africa*

⁷*iThemba LABS, Somerset West 7129, South Africa*

(Received 2 October 2013; published 27 November 2013)

High-energy-resolution $^{56}\text{Fe}(^3\text{He}, t)^{56}\text{Co}$ reaction measurements were performed at forward angles including 0° . From the spectra obtained, the splitting of the Fermi transition strength and thus the isospin mixing between the $J^\pi = 0^+$ isobaric analog state (IAS) at 3.60 MeV and a neighboring 0^+ state at 3.53 MeV have been investigated. In order to distinguish between states excited in Fermi and Gamow-Teller (GT) transitions, the measurements were performed at two ^3He beam energies of 140 and 100 MeV/nucleon. Owing to the different incident energy dependencies of the $\sigma\tau$ - and τ -type effective interaction strengths, it is expected that the Fermi transitions are stronger relative to GT transitions at lower beam energies. Therefore the excitation of a state by the Fermi transition could be identified by the $\Delta L = 0$ angular distribution and the ratio of transition strengths at these two incident energies. In the energy region around the IAS at 3.60 MeV, it was found that the state at 3.53 MeV is also excited by the Fermi transition and thus it has J^π values of 0^+ . A value of 32.3(5) keV could be deduced for the off-diagonal matrix element of the Hamiltonian that causes the isospin mixing. A corresponding isospin impurity of $28 \pm 1\%$ was obtained.

DOI: [10.1103/PhysRevC.88.054329](https://doi.org/10.1103/PhysRevC.88.054329)

PACS number(s): 21.10.Hw, 21.10.Re, 25.55.Kr, 27.40.+z

I. INTRODUCTION

The Fermi transition connects the initial state in a parent nucleus and the isobaric analog state (IAS) in the daughter nucleus having the same structure and quantum numbers J^π and isospin T , although the third component of isospin $T_z = (N - Z)/2$ is different by one unit. If the Fermi transition strength is shared between states having nominally different values of isospin T , it will provide direct information on isospin mixing. Such mixing is caused by the off-diagonal matrix element of the charge-dependent part of the Hamiltonian, which will be denoted by $\langle \mathcal{H}_C \rangle$.

In light and medium mass nuclei, typical values of $\langle \mathcal{H}_C \rangle$ of around 20 keV or less were deduced from β -decay measurements of Fermi transitions to isospin-forbidden states [1]. In studies of ^{24}Al , ^{57}Ni , and ^{64}Ga , however, larger values of $\langle \mathcal{H}_C \rangle = 106(40)$, $54(10)$, and $41.7(11)$ keV, respectively, were reported [2–4].

Studies of isospin-forbidden transitions in nuclear charge exchange (CE) reactions are also potentially powerful tools to

study isospin impurity. For medium and heavy mass nuclei, isospin mixing of the IAS was studied systematically from the broadening of the IAS peak in high-resolution ($^3\text{He}, t$) reaction studies [5]. For lighter nuclei, such as those in the pf shell, where the level density is not high, it is expected that a fragmentation or splitting of the IAS strength can be studied. If the IAS is associated with a nearby state having the same J^π values but a different nominal value of T , then the Fermi transition to the nearby state becomes possible due to the mixture of isospin induced by $\langle \mathcal{H}_C \rangle$.

Studies with the (p, n) -type CE reactions on ^{56}Fe allowed the isospin mixing between the $T = 2$, $J^\pi = 0^+$ IAS in ^{56}Co and the nearby $T = 1$, 0^+ state to be investigated [6,7]. In the $^{56}\text{Fe}(^3\text{He}, t)^{56}\text{Co}$ reaction at $E = 24.6$ MeV, Dzubay *et al.* [6] observed two peaks at excitation energies of 3.533 and 3.592 MeV in ^{56}Co . They made tentative assignments of $J^\pi = 0^+$ with isospin $T = 1$ and 2 for these states, respectively. The value of $\langle \mathcal{H}_C \rangle$ was estimated to be 33(3) keV. Similarly, Orihara *et al.* [7] reported an $\langle \mathcal{H}_C \rangle$ value of ≈ 50 keV using the $^{56}\text{Fe}(p, n)^{56}\text{Co}$ reaction at $E_p = 17$ MeV.

However, at these low incident energies the proportionality between the squared value of the transition matrix element and the reaction cross section is questionable due to a non-negligible multistep component in the reaction mechanism. In order to avoid such empirical ambiguities, measurements at intermediate incident energies ($E \geq 100$ MeV/nucleon) are required. However in the $^{56}\text{Fe}(p, n)^{56}\text{Co}$ measurement at $E_p = 160$ MeV reported in Ref. [8], the energy resolution was not good enough to resolve the IAS and the nearby 0^+ state.

*hfujita@rcnp.osaka-u.ac.jp; also at Research Center for Nuclear Physics (RCNP), Ibaraki, Osaka 567-0047, Japan.

[†]Present address: National Institute of Radiological Sciences (NIRS), Chiba 263-8555, Japan.

[‡]Present address: Cyclotron and Radioisotope Center (CYRIC), Tohoku University, Aoba-ku, Sendai, Miyagi 980-8578, Japan.

[§]Present address: RIKEN Nishina Center, Wako, Saitama 351-0198, Japan.

At the Research Center for Nuclear Physics (RCNP) in Osaka, we could overcome these difficulties by using the high-resolution capability of the (${}^3\text{He}, t$) reaction. By applying lateral and angular dispersion matching conditions, an energy resolution typically less than 30 keV can be achieved even at the intermediate incident beam energy of 140 MeV/nucleon [9]. At this energy, we believe that multistep reactions are small and good proportionality is expected between the 0° cross sections and the square of the transition matrix elements [10–12].

II. EXPERIMENT

The ${}^{56}\text{Fe}({}^3\text{He}, t){}^{56}\text{Co}$ experiments were performed at RCNP using 140 and 100 MeV/nucleon beams of ${}^3\text{He}$ from the Ring Cyclotron [13]. The WS beamline [14], designed to realize full dispersion matching with the Grand Raiden magnetic spectrometer, was used to transport a ${}^3\text{He}$ beam onto the target. In order to achieve high energy resolution and horizontal scattering angle resolutions, we applied lateral and angular dispersion matching conditions [15]. The dispersion matching conditions were realized by using the faint beam method [16] during the beam tuning procedure. A self-supporting ${}^{56}\text{Fe}$ foil with an areal density of 1.05 mg/cm² was used. Outgoing tritons were momentum analyzed by the Grand Raiden magnetic spectrometer [17]. The horizontal and vertical angular acceptances were ± 20 and ± 40 mr, respectively, defined by the rectangular shaped collimator installed at the entrance of the spectrometer.

Data were taken at laboratory angles of 0° , 2.5° , and 4° at a beam energy of 140 MeV/nucleon and at 0° at 100 MeV/nucleon. During the measurements at 0° , the ${}^3\text{He}^{2+}$ ion beam was stopped by a Faraday cup (FC) placed inside the first dipole magnet of the spectrometer. For the measurements at 2.5° and 4° , the FCs installed at the first quadrupole magnet of the spectrometer [18] and in the collimator box of the spectrometer, respectively, were used. The tritons were detected by a pair of multiwire drift chambers (MWDCs) [19] placed along the focal plane at an angle of 45° relative to the central ray of the spectrometer. Each of them consists of two anode wire planes in which the sense wires are stretched at different angles for the position and angle measurements of incident particles in both the horizontal and vertical directions. Two layers of ΔE plastic scintillation detectors were installed downstream of the MWDCs for particle identification and the generation of fast timing signals.

To achieve a good angular resolution in the vertical direction, the off-focus mode [20] was applied. Due to the good angular resolution, kinematic defocusing effects in the horizontal and vertical directions were observed and could be corrected by software. After correcting these aberrations in the off-line analysis, excellent energy resolutions of 19 keV ($\Delta E/E = 4.5 \times 10^{-5}$) and 33 keV (11×10^{-5}) were achieved at 140 and 100 MeV/nucleon, respectively. The spectra for the scattering angle $\Theta < 0.5^\circ$ taken at the two beam energies are shown in Fig. 1 for the energy range of 2.5–4 MeV.

The calibration of excitation energies in the daughter nucleus was performed with the help of kinematic calculations using well-known discrete states observed in the ${}^{\text{nat}}\text{Si}({}^3\text{He}, t)$ spectrum taken under the same conditions as the

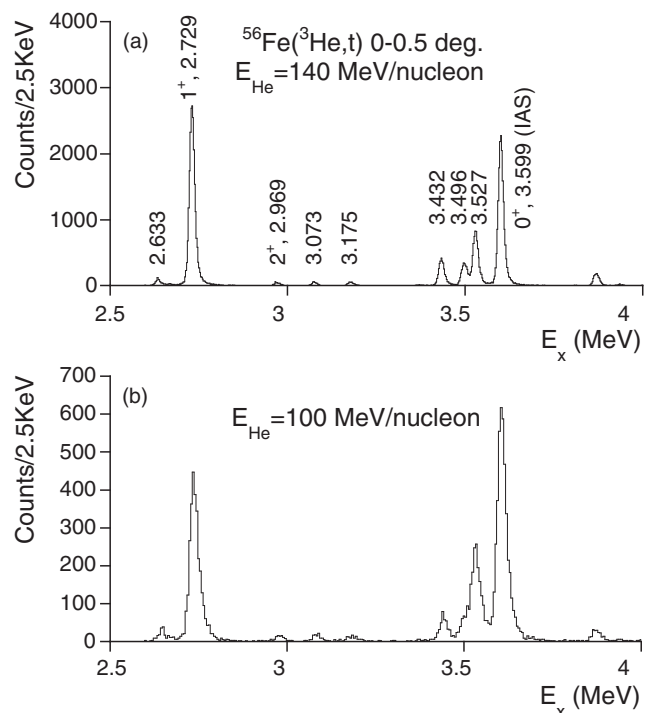


FIG. 1. Excitation energy spectra of ${}^{56}\text{Fe}({}^3\text{He}, t)$ reaction from 2.5 to 4 MeV at incoming ${}^3\text{He}$ energies of (a) 140 MeV/nucleon and (b) 100 MeV/nucleon, respectively. Events with scattering angles $\Theta < 0.5^\circ$ are included. Values of the excitation energies obtained in the present analysis are shown.

${}^{56}\text{Fe}$ measurement. Known excitation energies of states up to 4 MeV in ${}^{56}\text{Co}$ [21] were reproduced to within 10 keV, where differences between the reconstructed excitation energies and the known values in Table I are randomly distributed. In order to obtain peak intensities, the spectra were analyzed with peak deconvolution software [22], in which the experimental peak shape of the strongly excited and well-isolated Gamow-Teller (GT) state was used as a reference.

III. DATA ANALYSIS

According to Ref. [6], the excited state at 3.527 MeV is the most probable candidate for the $T = 1, 0^+$ state. However, since many 0^+ candidates have been reported in the ${}^{56}\text{Co}$ nucleus between 3 and 4 MeV [21], we decided to perform an independent J^π identification.

The transition to the $J^\pi = 0^+$ IAS is caused by a Fermi (τ) interaction and, therefore, is characterized by $\Delta L = 0$, $\Delta S = 0$, and $\Delta T = 1$. On the other hand, the transitions to 1^+ states are mainly of Gamow-Teller ($\sigma\tau$) type and they are characterized by $\Delta L = 0$, $\Delta S = 1$, and $\Delta T = 1$. These $\Delta L = 0$ transitions can be identified by the characteristic shape, peaked at 0° , of the angular distribution of the reaction cross sections.

In Fig. 2, angular distributions of reaction cross sections for the 0^+ IAS at 3.599 MeV and the neighboring states at 3.432, 3.496, and 3.527 MeV, studied in the (${}^3\text{He}, t$) reaction at 140 MeV/nucleon, are shown. As an example of the typical $\Delta L = 0$ transition, the angular distribution of the well-known

TABLE I. Excitation energies of states in the 2.5–4 MeV region, ratios of cross sections at 140 and 100 MeV/nucleon for the $\Delta L = 0$ states, and results of J^π identification.

From Ref. [21]		Present data			J^π
E_x (MeV)	J^π	E_x (MeV)	ΔL	Ratio ^a	
2.63564(19)	1^+	2.633	2		
2.6472(7)	$(0^+, 1^+)$				
2.72989(15)	1^+	2.729	0	1	1^+
2.969(5)	2^+	2.969	2		
3.07591(22)	1^+	3.073	(0)		
3.180(5)	$1^+, 3^+$	3.175	2		
3.234(5)	0^+				
3.378(10)	1^+				
3.436(5)	$0^+, 1^+$	3.432	0	0.97(14)	1^+
3.493(5)		3.496	0	1.09(14)	1^+
3.510(11)	(0^+)				
3.5266(5)	0^+	3.527	0	1.91(15)	0^+
3.59864(23)	$0^+, 1^+$	3.599	0	1.85(12)	0^+
3.807(10)	$1^+, 2^+, 3^+$				
3.863(12)		3.870	0	1.07(8)	1^+

^aThe ratio of the 2.729 MeV state is normalized to unity (see text).

$J^\pi = 1^+$ state at 2.729 MeV is also shown. For the IAS and the GT state at 2.729 MeV, the typical 0° peak of the angular distributions was confirmed. In addition, the $\Delta L = 0$ nature of the other states is obvious from the similar 0° peaked angular distributions.

In order to further distinguish the 0^+ and 1^+ nature of these states, we can use the fact that the strengths of the τ -type and $\sigma\tau$ -type effective interactions have different dependencies on the incoming energy of the projectile [10–12]. As mentioned above, in charge exchange reactions at intermediate energies and near 0° , there is a good proportionality between the GT and Fermi reaction cross sections and the squared transition matrix elements, and thus the GT and Fermi reduced transition

strengths, $B(\text{GT})$ and $B(\text{F})$, respectively:

$$\sigma_{\text{GT}}(0^\circ) = \hat{\sigma}_{\text{GT}} B(\text{GT}), \quad (1)$$

$$\sigma_{\text{F}}(0^\circ) = \hat{\sigma}_{\text{F}} B(\text{F}), \quad (2)$$

where $\hat{\sigma}_{\text{GT}}$ and $\hat{\sigma}_{\text{F}}$ denote GT and Fermi unit cross sections, respectively. It should be noted that $B(\text{GT})$ and $B(\text{F})$ are proportional to the squared GT and Fermi transition matrix elements. A systematic study in (p, n) reactions below $E_p = 200$ MeV showed that the ratio of the unit cross sections $\hat{\sigma}_{\text{GT}}/\hat{\sigma}_{\text{F}}$ is almost proportional to the squared value of the incoming energy of the proton beam [10]. This has been explained by the fact that the strength of the τ term of the free nucleon-nucleon interaction becomes larger at lower incident energies, while the strength of the $\sigma\tau$ term remains nearly the same [11]. Therefore it is suggested that $\hat{\sigma}_{\text{F}}$ will become larger relative to $\hat{\sigma}_{\text{GT}}$ at lower incoming energies and thus the Fermi states will be enhanced relative to the GT states in the spectra obtained.

The $^{56}\text{Fe}(^3\text{He}, t)$ spectra at 140 and 100 MeV/nucleon are compared in Fig. 1, where the ordinates of the spectra are adjusted so that the 1^+ state at 2.729 MeV has nearly the same height. As is clear, the 3.599-MeV IAS is enhanced in the spectrum taken at 100 MeV/nucleon. In addition, it should be noted that the 3.527-MeV state is also enhanced.

In Table I, the E_x , ΔL , and J^π values assigned in this work are summarized for the states observed in this measurement. The ratios of the cross sections at 100 and 140 MeV/nucleon were obtained for the $\Delta L = 0$ states from the spectra at scattering angles $\Theta < 0.5^\circ$. The isolated strong GT state at 2.729 MeV was used as the normalization standard. Therefore, the ratios show how much the relative cross sections increase in the measurement at 100 MeV/nucleon compared to that at 140 MeV/nucleon. Statistical errors and ambiguities in the peak deconvolution analysis were taken into account.

For the states at 3.432 and 3.496 MeV, ratios of 0.97(14) and 1.09(14) were obtained, respectively. These values are unity within uncertainties and suggest that these states are excited by $\sigma\tau$ -type interactions and, therefore, have $J^\pi = 1^+$. On the other hand, as was expected, an enhanced ratio of 1.85(12) was obtained for the IAS at 3.599 MeV. In addition, the state at 3.527 MeV, the nearest state to the IAS, exhibited a ratio of 1.91(15), which is in good agreement with that for the IAS. From this result, we conclude that this state is also excited via a τ -type operator and therefore has $J^\pi = 0^+$, which is consistent with Ref. [6]. The lower excitation energy of this state compared with that of the IAS implies that this state has the nominal isospin of $T = 1$. These facts suggest that this 0^+ state is excited through the isospin impurity part ($T = 2$) of the wave function caused by the isospin mixing and carries part of the Fermi transition strength.

By assuming that the total Fermi transition strength $B(\text{F})$ of $N - Z = 4$ is shared by the IAS at 3.599 MeV and the 0^+ state at 3.527 MeV, it was deduced that $B(\text{F})$ values are 2.89(12) and 1.11(6), respectively.

IV. ISOSPIN MIXING MATRIX ELEMENT

If the splitting of the Fermi transition strength is caused by the isospin mixing between the two $J^\pi = 0^+$ states with

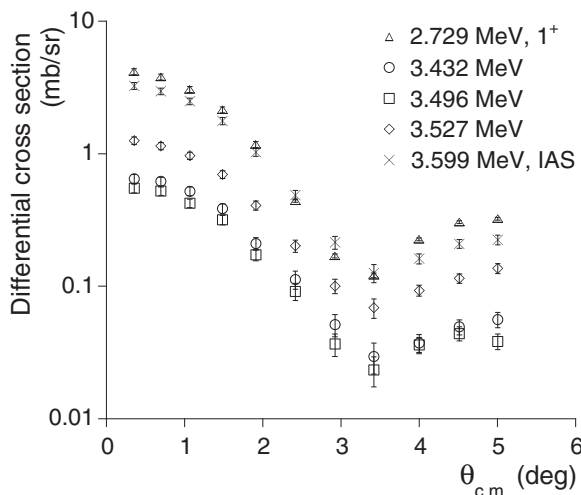


FIG. 2. Obtained angular distributions of the IAS at 3.599 MeV and neighboring excited states at an incoming ^3He energy of 140 MeV/nucleon.

$T = 2$ and 1, then the off-diagonal part of the Hamiltonian can be deduced. We write the ^{56}Co nuclear Hamiltonian \mathcal{H} as

$$\mathcal{H} = \mathcal{H}_0 + \mathcal{H}_C, \quad (3)$$

where \mathcal{H}_0 is the charge-independent part of the Hamiltonian. Therefore, its eigenstates have isospin as a good quantum number. Since isospin is a reasonably good quantum number, we assume that \mathcal{H}_0 is the main part of the total Hamiltonian and it is diagonalized. On the other hand, the charge-dependent part of the Hamiltonian \mathcal{H}_C can mix different eigenstates of \mathcal{H}_0 by the off-diagonal matrix elements.

Two eigenstates Φ_a and Φ_b of \mathcal{H}_0 , having isospin values of $T = 2$ and 1, satisfy the relationships

$$\begin{cases} \mathcal{H}_0 \Phi_a = e_a \Phi_a, \\ \mathcal{H}_0 \Phi_b = e_b \Phi_b. \end{cases} \quad (4)$$

The energies E_a and E_b of the observed states are eigenvalues of the total Hamiltonian \mathcal{H} and the actual wave functions Ψ_a and Ψ_b satisfy

$$\begin{cases} (\mathcal{H}_0 + \mathcal{H}_C)\Psi_a = E_a \Psi_a, \\ (\mathcal{H}_0 + \mathcal{H}_C)\Psi_b = E_b \Psi_b. \end{cases} \quad (5)$$

We write the states Ψ_a and Ψ_b in terms of linear combinations of the two states Φ_a and Φ_b :

$$\Psi_a = \beta \Phi_a + \alpha \Phi_b, \quad (6)$$

$$\Psi_b = -\alpha \Phi_a + \beta \Phi_b, \quad (7)$$

where $\alpha^2 + \beta^2 = 1$ and therefore α^2 represents the isospin impurity. By using these relationships, the off-diagonal matrix element of the charge-dependent part of the Hamiltonian $\langle \mathcal{H}_C \rangle$ can be written as

$$\langle \mathcal{H}_C \rangle = \langle \Phi_a | \mathcal{H}_C | \Phi_b \rangle = \alpha\beta(E_a - E_b). \quad (8)$$

The final states Ψ_a and Ψ_b correspond to the IAS and the nearby 0^+ state, in which wave functions Φ_a and Φ_b with $T = 2$ and 1, respectively, are mixed via $\langle \mathcal{H}_C \rangle$. On the other hand, in the initial ^{56}Fe ground state, such mixing cannot happen because states in ^{56}Fe can never have $T = 1$ due to the T_z value of $+2$. Thus, the ^{56}Fe ground state is expected to be described by Φ_a except for the different T_z value. Hence the ratio of the two Fermi-transition cross sections can be expressed as

$$\frac{d\sigma_b / d\Omega}{d\sigma_a / d\Omega} = \frac{B(\text{F})_b}{B(\text{F})_a} \quad (9)$$

$$= \frac{| \langle 0^+, 3.527 | \tau_- | ^{56}\text{Fe g.s.} \rangle |^2}{| \langle \text{IAS}, 3.599 | \tau_- | ^{56}\text{Fe g.s.} \rangle |^2} \quad (10)$$

$$= \frac{| \langle \Psi_b | \tau_- | \Phi_a(T_z = +2) \rangle |^2}{| \langle \Psi_a | \tau_- | \Phi_a(T_z = +2) \rangle |^2} \quad (11)$$

$$= \left(\frac{\alpha}{\beta} \right)^2, \quad (12)$$

where we used the fact that $B(\text{F})$ is proportional to the squared value of the transition matrix element.

As a result, an isospin impurity of $\alpha^2 = 28(1)\%$ was found, and by applying Eq. (8), the off-diagonal matrix element of

$$\langle \mathcal{H}_C \rangle = 32.3(5) \text{ keV}$$

was obtained; these are consistent with values from Refs. [6,7].

From the high-resolution $^{41}\text{K}(^3\text{He}, t)^{41}\text{Ca}$ study at 140 MeV/nucleon, $\langle \mathcal{H}_C \rangle \approx 8$ keV was obtained for $A = 41$ nuclei by analyzing the difference of the strengths of two nearby GT transitions [23]. It should be noted that rather different $\langle \mathcal{H}_C \rangle$ values are also given in the compilation in Ref. [1], as mentioned above. For understanding these differences, further studies are needed.

V. CONCLUSION

We have performed high-resolution $^{56}\text{Fe}(^3\text{He}, t)$ experiments at two different incident energies of 140 and 100 MeV/nucleon. The energy resolutions of 19 and 33 keV made it possible to study the fine structure of the excited states close to the IAS. Both GT and Fermi transitions have a $\Delta L = 0$ nature. The GT and Fermi reaction cross sections, however, have a different dependence on the incident beam energy; the Fermi excitation is stronger at 100 MeV/nucleon than at 140 MeV/nucleon relative to the GT excitations. It was found that both the IAS (nominal $T = 2$) at 3.599 MeV and the nearby state (nominal $T = 1$) at 3.527 MeV show $\Delta L = 0$ angular distributions and have such incident energy dependencies. It is strongly suggested that both states are excited by the Fermi transition and therefore have $J^\pi = 0^+$. A value of 32.3(5) keV was obtained for the off-diagonal matrix element of the Hamiltonian.

ACKNOWLEDGMENTS

The $^{56}\text{Fe}(^3\text{He}, t)$ experiments were performed at RCNP under the Experimental Programs E252 and E338. We are grateful to the RCNP accelerator group for their effort in providing a high-quality ^3He beam at both 140 and 100 MeV/nucleon. The high quality of the beam was indispensable for the realization of the matching conditions. HF and YF appreciate discussions with Prof. S. Sasaki (CQST, Osaka University) in the data analysis on isospin mixing. HF and YF

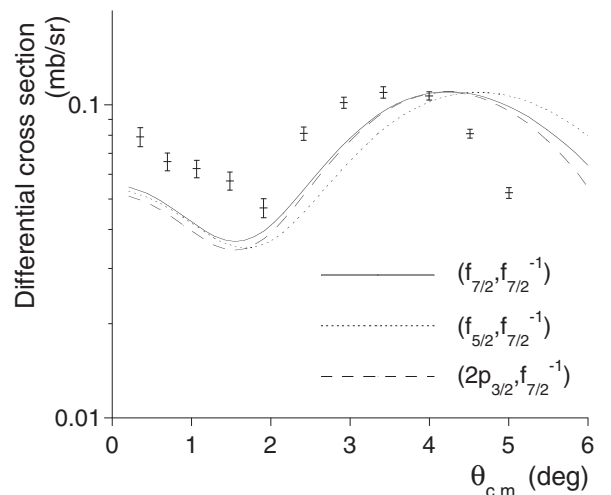


FIG. 3. Angular distribution of measured cross sections for the 2^+ state at 2.969 MeV at an incoming ^3He energy of 140 MeV/nucleon and those obtained by DWBA calculations.

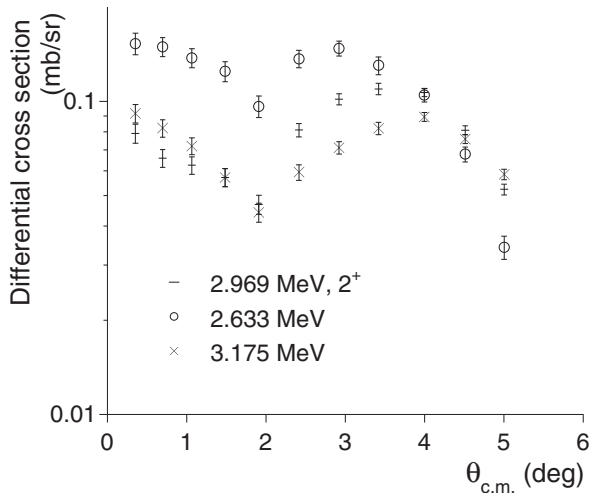


FIG. 4. Angular distributions of states at 2.633, 2.969, and 3.175 MeV at an incoming ^3He energy of 140 MeV/nucleon.

acknowledge the discussion with Prof. W. Gelletly (Surrey) on preparation of this paper. This work was in part supported by Monbukagakusho, Japan, under Grants No. 18540270 and No. 22540310.

APPENDIX: J^π ASSIGNMENTS FOR THE WEAKLY EXCITED STATES

As shown in Fig. 1, we see several weakly excited states. From the analysis of the angular distributions, the J^π values for these states assigned in Ref. [21] were examined.

In Fig. 3, we compare the angular distribution for the 2^+ state at 2.969 MeV with the distorted wave Born approximation (DWBA) calculations assuming $J^\pi = 2^+$ with pure $(f_{7/2}, f_{7/2}^{-1})$, $(f_{5/2}, f_{7/2}^{-1})$, and $(2p_{3/2}, f_{7/2}^{-1})$ configurations, respectively. The calculated cross sections were normalized so as to have the same peak value as the measured value. Reasonably good agreement of the shape suggests a $\Delta L = 2$ nature for this state, which is consistent with the assigned J^π values of 2^+ .

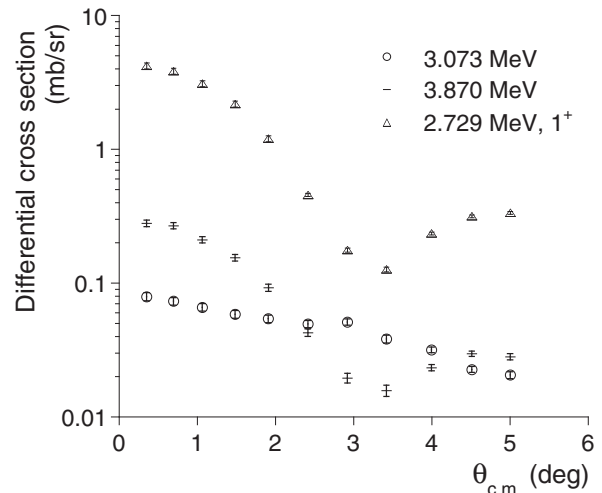


FIG. 5. Angular distributions of states at 3.073, 3.870, and 2.729 MeV at an incoming ^3He energy of 140 MeV/nucleon.

For the 2.633- and the 3.175-MeV states, J^π values of 1^+ and 1^+ or 3^+ were assigned, respectively. In Fig. 4, the angular distributions obtained for these states are compared with that for the 2^+ state at 2.969 MeV. The similarities in the angular distributions suggest that they also have a dominant $\Delta L = 2$ character.

In Fig. 5, the angular distributions for the states at 3.073 MeV, 1^+ , and 3.870 MeV are shown. The angular distribution of the well-known 1^+ state at 2.729 MeV is also shown as a reference. For the state at 3.870 MeV, no J^π value assignment is available in Ref. [21]. The similarity of the angular distribution to that of the 2.729-MeV state suggests a $\Delta L = 0$ nature for this transition. In addition, due to the strength ratio of 1.07(8) at 140 and 100 MeV/nucleon (see Table I), we suggest the 1^+ assignment for this state. For the 3.073-MeV state, assigned J^π values of 1^+ would be reliable since γ decays to the 2^+ states at 0.970 and 2.060 MeV and the 0^+ state at 1.451 MeV are reported [21]. The angular distribution peaks at a smaller angle; however, it is quite different from that of the 2.729-MeV state.

-
- [1] S. Raman, T. A. Walkiewicz, and H. Behrens, *At. Data Nucl. Data Tables* **16**, 451 (1975), and references therein.
- [2] C. D. Hoyle, E. G. Adelberger, J. S. Blair, K. A. Snover, H. E. Swanson, and R. D. Von Lintig, *Phys. Rev. C* **27**, 1244 (1983).
- [3] J. Atkinson, L. G. Mann, K. G. Tirsell, and S. D. Bloom, *Nucl. Phys. A* **114**, 143 (1968).
- [4] S. Raman, N. B. Gove, and T. A. Walkiewicz, *Nucl. Phys. A* **254**, 131 (1975).
- [5] J. Jänecke, M. N. Harakeh, and S. Y. van der Werf, *Nucl. Phys. A* **463**, 571 (1987), and references therein.
- [6] T. G. Dzubay, R. Sherr, F. D. Becchetti, Jr, and D. Dehnhard, *Nucl. Phys. A* **142**, 488 (1970).
- [7] H. Orihara, K. Ogawa, T. Murakami, S. Nishihara, T. Nakagawa, and K. Maeda, *Nucl. Phys. A* **403**, 317 (1983).
- [8] J. Rapaport *et al.*, *Nucl. Phys. A* **410**, 371 (1983).
- [9] Y. Fujita, B. Rubio, and W. Gelletly, *Prog. Part. Nucl. Phys.* **66**, 549 (2011).
- [10] T. N. Taddeucci, C. A. Goulding, T. A. Carey, R. C. Byrd, C. D. Goodman, C. Gaarde, J. Larsen, D. J. Horen, J. Rapaport, and E. Sugarbaker, *Nucl. Phys. A* **469**, 125 (1987), and references therein.
- [11] F. Osterfeld, *Rev. Mod. Phys.* **64**, 491 (1992), and references therein.
- [12] J. Rapaport and E. Sugarbaker, *Annu. Rev. Nucl. Part. Sci.* **44**, 109 (1994).
- [13] I. Miura *et al.*, RCNP (Osaka University) Annual Report, 1991 (unpublished), p. 149, <http://www.rcnp.osaka-u.ac.jp>.
- [14] T. Wakasa *et al.*, *Nucl. Instrum. Methods Phys. Res., Sect. A* **482**, 79 (2002).

- [15] Y. Fujita, K. Hatanaka, G. P. A. Berg, K. Hosono, N. Matsuoka, S. Morinobu, T. Noro, M. Sato, K. Tamura, and H. Ueno, *Nucl. Instrum. Methods Phys. Res., Sect. B.* **126**, 274 (1997).
- [16] H. Fujita *et al.*, *Nucl. Instrum. Methods Phys. Res., Sect. A* **484**, 17 (2002).
- [17] M. Fujiwara *et al.*, *Nucl. Instrum. Methods Phys. Res., Sect. A* **422**, 484 (1999).
- [18] M. Itoh *et al.*, RCNP (Osaka University) Annual Report, 1999 (unpublished), p. 7.
- [19] T. Noro *et al.*, RCNP (Osaka University) Annual Report, 1991 (unpublished), p. 177.
- [20] H. Fujita *et al.*, *Nucl. Instrum. Methods Phys. Res., Sect. A* **469**, 55 (2001).
- [21] H. Junde, H. Su, and Y. Dong, *Nucl. Data Sheets* **112**, 1513 (2011).
- [22] H. Fujita *et al.*, RCNP (Osaka University) Annual Report, 2010 (unpublished), p. 3.
- [23] Y. Fujita *et al.*, *Phys. Rev. C* **70**, 054311 (2004).